Through Hydrogen-Bond Vibrational Coupling in Hydrogen-Bonding Chains of 4-Pyridones with Implications for Peptide Amide I Absorptions: Density Functional Theory Compared with Transition Dipole Coupling

Yung-fou Chen,[†] Raji Viswanathan,[‡] and J. J. Dannenberg*,[†]

Department of Chemistry and Biochemistry, City University of New York— Hunter College and the Graduate School, 695 Park Avenue, New York, New York 10021, and Department of Chemistry Yeshiva College, 500 West 185th Street, New York, New York 10033

Received: April 3, 2007; In Final Form: May 7, 2007

We present B3LYP/D95** calculations on the C═O and N−H couplings in H-bonded chains of 4-pyridones. ^{14}C-substitutions are used to decouple various vibrations for purposes of illustration. The coupled C═O vibrations bear analogy to the amide I bands of proteins and peptides. The coupling of the C═O's occurs primarily via the cooperative H-bonds rather than transition dipole coupling (TDC), as demonstrated by the fact that (1) the couplings are greater than previously reported for similar studies on formamides despite the larger distance between the C═O's in the pyridone chains (TDC coupling decreases with distance) and (2) the red shifts (also greater than for formamides) can be attributed to the changes in the geometries (particularly the C═O bond lengths) of the individual 4-pyridones in the H-bonding chains induced by the H-bonds and resulting polarization of the monomers.

Nature has made extensive use of the N−H···O═C H-bonding motif in various guises to form self-assembled biomaterials. She has used a paradigm of multiple complementary H-bonding arrays in nucleic acids where the specific base pairs are complementary in their H-bonding donors/acceptors and in size (only one purine + one pyrimidine can fit across the backbones) to form stable structures. This paradigm has been successfully applied to many self-assembling systems (we cite only a small selection of representative reports).[1−4] She has used a different paradigm in the self-assembly of proteins. Unlike the nucleic acids, which allow relatively little structural variation, proteins can form an almost limitless number of stable structures, in principle. If all of the N−H···O═C H-bonds be energetically equivalent, then the peptides structures must be dictated entirely by other factors, be they steric, hydrophobic, covalent (sulfur bridges), or electrostatic (between ionized side chains and/or other ions). However, this particular kind of H-bond can have an unusually wide range of energies depending upon its environment as it is subject to enormous amounts of cooperative interactions.

The remarkable C═O···H−N H-bond can achieve enthalpies of association from about 2 kcal/mol (in one of the dimers of a diglycine)[5] to 23 kcal/mol in the centermost H-bonds of chains of 4-pyridones.[6] Cooperative H-bond interaction plays an important role in the modulating the magnitude of H-bonding interactions.[7] Coupling between the C═O's in proteins and peptides results in the amide I infrared absorption often used to characterize these molecules. The coupling involved in the amide I band can occur by through-space transition dipole coupling (TDC) or by coupling of the C═O's mediated by H-bonds. The TDC method of calculating the coupling between C═O's in peptides was introduced by Krimm.[8] The coupling between the oscillators is based upon the electrostatic interactions between the oscillating dipoles. As dipole−dipole interactions are electrostatic in nature, the mechanism of TDC depends upon the predominance of electrostatics in determining the interaction between the coupled entities. The failure of electrostatic interactions to predict the cooperativity of H-bonds in peptides[9−12] and in molecular crystals[13−16] has long been established. The importance of vibrational coupling of C═O's through the H-bonds in H-bonding formamide chains,[17] dimers and trimers of N-methylformamide,[18] and in infinite α-helices have been noted in the literature.[19] However, many reports continue to ignore this important effect. In this paper, we use H-bonding chains of 4-pyridones to demonstrate the importance of coupling C═O's through H-bonds.

Chains of 4-pyridones (see Figure 1) provide the strongest single C═O···H−N H-bonds between neutral species of which we are aware.[6] Thus, the effect of C═O coupling through H-bonds should be magnified in 4-pyridone H-bonding chains relative to peptides, rendering the demonstration of this effect more evident. In contrast, larger distance between C═O's will reduce the magnitude of the TDC from that expected from peptides. Both the monomers and the chains attain structures with C_{2v} symmetry. Thus, the collinear C═O's have their individual transition dipoles aligned with each other and with the transition dipoles of the amide I vibrations of the aggregates.

The amide-II (C−N−H stretch/bend) and amide-A (N−H stretch) also provide structurally useful information on peptide structure. There is no vibration truly equivalent to the amide II band for H-bonding chains of 4-pyridones. However, the N−H stretches couple quite strongly. We shall also discuss these vibrations below.

Calculational Details

All the DFT calculations reported here used the B3LYP functional with the D95(d,p) basis set which we have shown to be appropriate for H-bonding interactions. This method com-

* Corresponding author. E-mail: jdannenberg@gc.cuny.edu.
[†] City University of New York.
[‡] Yeshiva College.

10.1021/jp072624y CCC: $37.00
Published on Web 06/22/2007

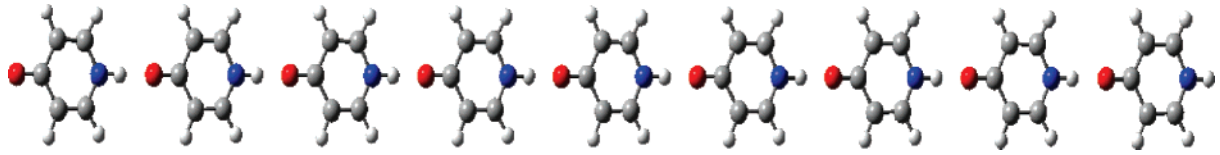

Figure 1. An H-bonding chain of nine 4-pyridones.

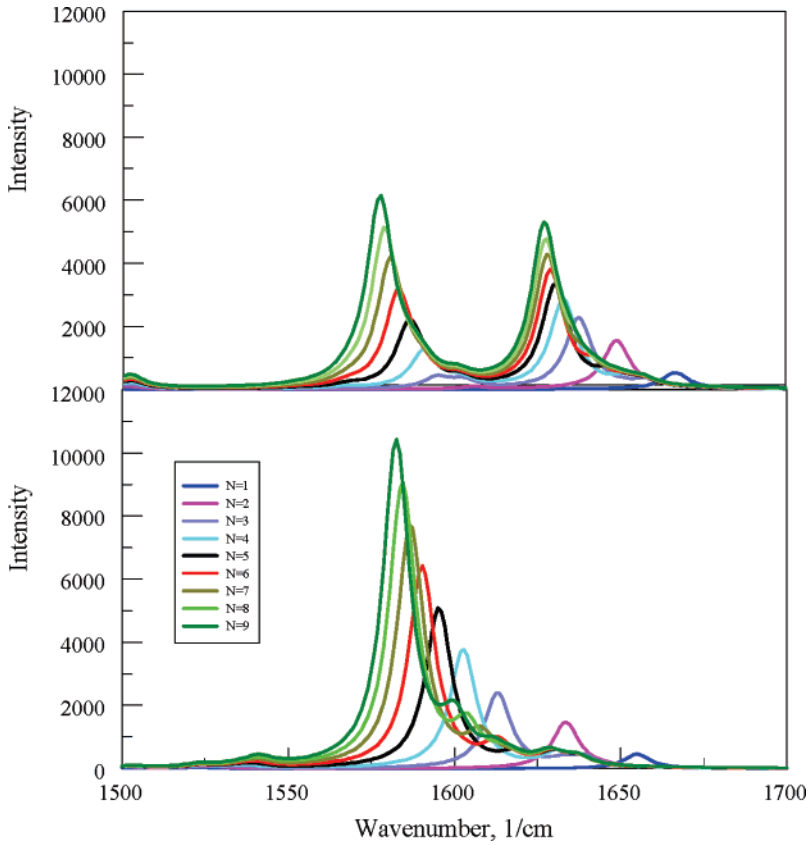

Figure 2. The C═O region of the IR spectrum for $(4\text{-pyridone})_N$. The lower panel shows the spectrum when all C═O's are substituted with ^{14}C.

bines Becke's 3-parameter functional,[20] with the nonlocal correlation provided by the correlation functional of Lee, Yang and Parr.[21] The geometries of the 4-pyridone chains were completely optimized within the constraint that they maintain a plane and an axis of symmetry. The vibrational frequencies used the harmonic approximation. All DFT calculations used the GAUSSIAN 03 suite of programs,[22] as in our previous study of vibrations in H-bonding chains of formamides. Through space dipole−dipole coupling (TDC) interactions are presented for comparison with the DFT results. These have been calculated from the Cartesian coordinates of only the carbons and oxygens of the C═O's taken from the same optimized geometries used for the DFT calculations. We used a program developed by Diem[23] for this purpose which incorporates procedures he described earlier. The transition dipoles are collinear with the C═O bonds as a result of the symmetry of the H-bonding chains.

The vibrational "frequencies" are reported as wavenumbers in cm^{-1}, which is more appropriately $1/\lambda$ than ν, (c/λ). While we strongly believe the practice of scaling frequencies to be inimical to the spirit of ab initio calculations, we realize that scaling makes the computed vibrations more easily comparable to those obtained experimentally by biochemists and spectroscopists. For this reason we have applied a scaling factor of 0.965, which we have previously found to be suitable for B3LYP/D95** and similar DFT calculations.[24,25] The original calculated frequencies can be obtained by dividing the scaled values by this factor.

We use ^{14}C substitution of the structures to selectively decouple vibrational modes. Substitution of four ^{14}C's in the two C═C bonds of each pyridone was used to decouple these stretching modes from those of the C═O to remove any ambiguity about which modes of the pyridones coupled in the aggregates. We (separately) decoupled individual C═O's in the nonamer to obtain the stretching modes of individual C═O's within the aggregate to illustrate the relationship between the C═O bond length variation and the C═O frequencies.

Results and Discussion

Figure 2 depicts the C═O stretching region of the IR spectra for 4-pyridone and aggregates containing from two to nine monomers. The upper part shows the spectra of the unsubstituted aggregates, while the lower part illustrates the spectra of the tetra-^{14}C substituted aggregates. The ^{14}C substitutions clearly remove the coupling observed in the upper spectra. We shall refer to the decoupled spectra in the lower part of the figure for the remaining discussion. The most intense absorption for all aggregates involves synchronous stretching of all C═O's. This absorption both increases in intensity and becomes more red-shifted as the aggregate becomes larger. The extents of these changes exceed the qualitatively similar changes previously reported for H-bonding chains of formamides,[17] as might be expected from the larger H-bonding energies reported for the pyridone[6] rather than formamide[10] H-bonding chains.

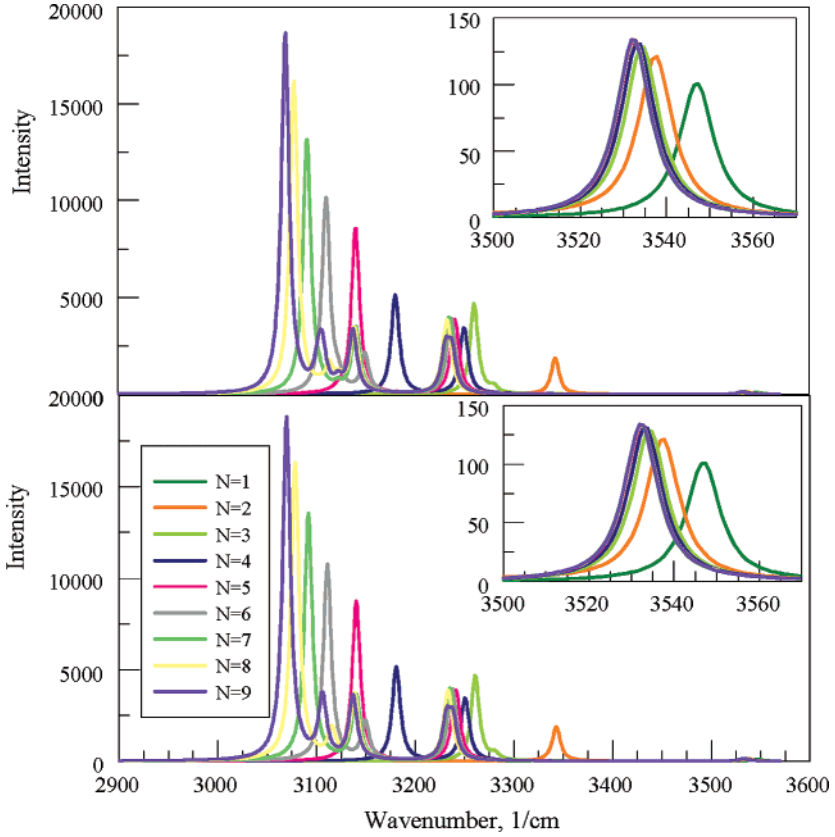

Figure 3. N−H stretching region of $(4\text{-pyridone})_N$. The lower panel shows the results for the chains where all four C−H's of the C═C bonds are substituted with C−D. The inset expands the part of the spectrum near 3500 cm^{-1}. The intensities are in km/mol.

The most intense, lowest-energy, and, therefore, most red-shifted C═O vibration for each chain involves the synchronous symmetric stretches of all the C═O's. The vibrational wavefunction for this mode would have no nodes. The next higher in energy belongs to the coupled mode where half of the C═O's on one end of the pyridone chain stretch synchronously in phase with each other, but out of phase with the other half. The vibrational wavefunction for this mode would have a node near the center of the chain. Thus, this mode should have little intensity. The third lowest-energy mode should have two nodes. This mode should have more intensity than the second lowest, but less than the lowest mode. Continuing in this manner, most of the intensity should be due to the odd numbered modes (counting from the lowest), and the intensity should fall off in these modes as the energy increases. Careful inspection of the figure reveals that a weak shoulder slightly blue-shifted from the most intense absorption appears for $N = 3$ or more. The chain of three is the smallest that can have two nodes in the vibrational wavefunction. This shoulder increases in intensity and becomes more red-shifted as N increases from three to nine in a manner similar to the most intense peak.

Figure 3 depicts the N−H stretching region of the same 4-pyridone chains. The upper part shows the this region for the isotopically unsubstituted molecules. The red shifts for the larger chains move the most intense N−H stretch into the region of the spectrum where C−H stretches might be expected. The lower part of the figure shows the same region for chains where all the C−H's have been replaced with C−D's to shift these vibrations out of the range of the IR spectrum covered in the figure. The observation that no substantial differences can be found between the two demonstrates that all the C−H vibrations are too weak to substantially alter the appearance of the N−H stretching absorptions. The approximately 500 cm^{-1} red shifts of the most prominent N−H stretch from that of the monomer and approximately 300 cm^{-1} from the H-bonded N−H in the dimer are significantly larger than normally expected for H-bonded N−H's. The intensity of the strongest absorption for $N = 9$ approaches 2000 times that for the monomer.

While the absorption spectra of the chains in the C═O and N−H regions have much in common (increasing red shift and intensity as the chain increases in length) several features distinguish them from one another. Most notably, the terminal N−H does not participate in an H-bond. It is largely unaffected by the growth of the H-bonding chain. It exhibits small red shifts that stop increasing when N exceeds 5. It shows only a modest increase in intensity which also stops when N reaches 5. Thus, the coupling really involves the N-1 N−H's that participate in the H-bonds. The most intense and red-shifted N−H stretch is for the completely symmetric stretch of the 8 H-bonded N−H for $N = 9$. In addition to the one very strong absorption, three others can be seen which correspond to the other vibrational wavefunctions that have an even number of nodes. Note that the least red-shifted of these coincides with absorptions from those chains with $N = 5$ or more. Thus this absorption appears to have reached its limiting value as N increases at $N = 5$. The next least red-shifted of the absorptions for $N = 9$ coincides with absorptions for $N = 7$ or more, suggesting that this absorption reaches its limiting value for $N = 7$. The two most red-shifted absorptions for $N = 9$ do not coincide with others, suggesting that these have not yet reached limiting values. Thus, red shifts larger than 500 cm^{-1} and higher intensities than 2000 times that of the monomer might be expected for longer chains.

We repeated the same vibrational coupling calculations using the TDC method. We set the reference frequency for these calculations to the scaled frequency of the 4-pyridone monomer

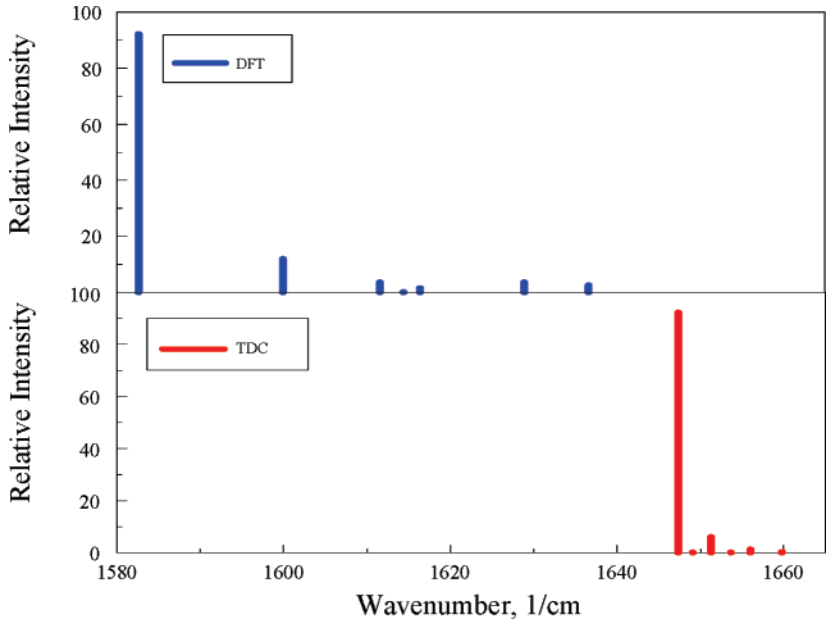

Figure 4. Individual C═O absorptions for (4-pyridone)$_9$ as calculated by DFT (above) and TDC (below). The DFT calculations refer to the H-bonding chain with ^{14}C═O's (to remove the coupling with the C═C's). The TDC frequencies are adjusted to match the scaled C═O stretching frequency of the monomeric 4-pyridone as calculated using DFT.

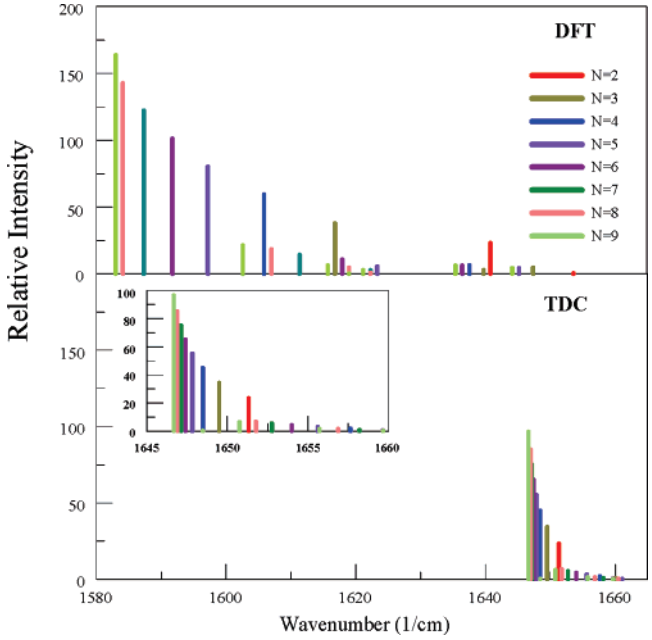

Figure 5. The individual C═O absorptions for (4-pyridone)$_N$ with four ^{14}C's as calculated by DFT (upper panel). and TDC (lower panel). The relative intensities are scaled to keep the intensity for $N = 2$ the same for both methods. The inset in the lower panel magnifies the scale.

(substituted with four ^{14}C's in the CdC bonds) as calculated by DFT (1655 cm^{-1}) so that the shifts calculated by the two methods could be compared. Figure 4 shows the individual C═O absorptions that comprise the amide-I band of (4-pyridone)$_9$ as calculated by DFT (upper part) and TDC (lower part). Figure 5 depicts all the absorptions of the amide-I region for each H-bonded chain.

In (4-pyridone)$_9$, the C═O's are so extensively coupled that one cannot assign a unique stretching frequency to each one. Nevertheless, each C═O is in a unique environment due to its position in the H-bonding chain. As expected from previous reports,[5,6,10−14,16,17,26] the H-bonding increases the C═O bond length. Those H-bonds nearest the center of the H-bonding chains, which participate in the strongest H-bonds, have the

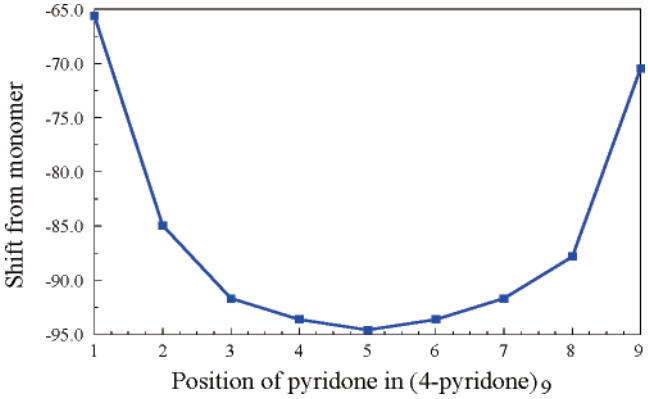

Figure 6. Shifts of the frequencies of the ^{14}C═O's the individually ^{14}C-substituted 4-pyridones in (4-pyridone)$_9$. The X-axis denotes which of the9 pyridones contains the ^{14}C═O.

longest C═O bonds. Since the C═O stretching frequency depends upon the strength of the bond, and since the bond length is generally a good indicator of C═O bond strength, one might expect the different C═O's in (4-pyridone)$_9$ to have different stretching frequencies were they not coupled. In order to probe these uncoupled C═O stretches, we decoupled individual C═O's in (4-pyridone)$_9$ by substituting one ^{14}C═O at a time for each of the nine unique 4-pyridones in the chain. Figure 6 shows the variation of the frequencies of the ^{14}C═O substituted 4-pyridones as a function of their position in the chain. Since the ^{14}C═O frequencies are necessarily red-shifted from the ^{12}C═O frequencies, they are plotted as the shift from the frequency of the ^{14}C═O substituted monomer. Red-shifts occur for all nine positions, even for the terminal 4-pyridone that does not form a H-bond with its C═O. The largest red-shifts occur in the more central monomers of (4-pyridone)$_9$. Figure 7 shows the ^{14}C═O frequencies plotted against the C═O bond lengths. The linear plot resembles those previously reported for formamide chains,[17] the relationship found for N-methylformamide hydrated by D_2O,[27] and the qualitative conclusions of Torii and Tusami in their study of N-methylfomamide dimers and trimers.[28] These data show the C═O bond lengthening upon

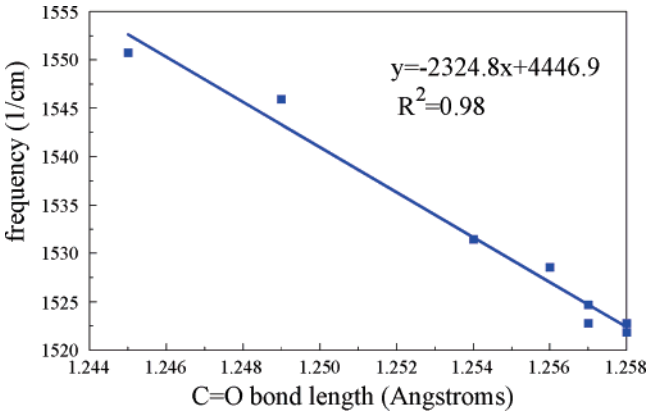

Figure 7. The frequency of the individually $^{14}C{=}O$ substituted 4-pyridones in $(4\text{-pyridone})_9$ plotted against the C═O bond length.

H-bonding to be a major contributor to the red-shifts of the C═O band of the $(4\text{-pyridone})_N$ chains.

Comparison of DFT with TDC. The observed couplings of the C═O stretches in the 4-pyridone chains differ from the expectations of TDC in several aspects:

(a) The distance dependence of dipole−dipole coupling cause the interaction to vary as the inverse cube of the distance between the dipoles. Since the interaction C═O dipoles are more distant from each other in the 4-pyridone chains than in the previously reported[17] formamide chains, TDC predicts less coupling for the 4-pyridones than for the formamides, contrary to our observations.

(b) TDC coupling predicts the center of the set of coupled absorptions to remain at the frequency of the single uncoupled oscillator (assuming they are equivalent, as is the case here). However, both the 4-pyridone and formamide chains show extensive red shifts of the center of the absorptions. In fact all of the absorption frequencies are red-shifted from that of the monomer. TDC cannot account for these shifts.

(c) The C═O bond lengths in the individual molecules within both the 4-pyridone and formamide chains vary with position and lengths of the chains. No mechanism exists for this geometry change in simple dipole−dipole coupling. Furthermore, the decoupled $^{14}C{=}O$'s frequencies correlate with the C═O bond lengths, for which TDC does not account.

(d) The relative intensities of the coupled C═O absorptions are not properly predicted by TDC. In particular, the most intense (and most red-shifted) absorption increase in relative intensity as the H-bonding chain grows in length much more rapidly than predicted by TDC for both the 4-pyridone and formamide chains.

On the other hand, all of these observations can be easily explained assuming the coupling occurs though the H-bonds:

(a) The coupling depends upon the strength of the H-bonds rather than the distance between the C═O's, as observed.

(b and c) The C═O's become more red-shifted as the H-bonding chain grows because the growing strengths of the cooperative H-bonding interactions shortens the H···O distances while lengthening (and weakening) the C═O bonds.

(d) Since the dipole moments of the 4-pyridone H-bonding chains increase much more rapidly than predicted by electrostatic interactions (i.e., vector addition of the dipole moments isolated of the individual 4-pyridones) due to the polarization that complements the H-bonding,[6] the transition dipoles (which determine the intensities of the individual absorptions - not to be confused with TDC) of the chains follow a similar trend.

Implications for Peptides and Proteins. While some reports of ab initio and DFT based vibrational analyses for some small peptides (too small to contain extensive cooperative H-bonding chains) have been reported,[28−38] biochemical vibrational spectroscopists have generally modeled the amide I band using though space dipole coupling of the relevant C═O's, often referred to as transition dipole coupling (TDC), either alone or in combination with other methods,[39] although several criticisms of TDC have appeared.[40−42] One very recent report calculates the coupling in the α-helical conformation of trialanine.[38] However, this conformation was not fully optimized as it is not even a local minmum,[11] and is too small for cooperative H-bonding. We shall describe our DFT based vibrational analyses of α-helical and β-sheet peptides elsewhere.

Electrostatic interactions between oscillators (or molecules) do not allow for reorganization of charge nor for reorganization of molecular interactions. Thus, the dipole moment of an ensemble of molecules or oscillating dipoles that interact purely by electrostatics would be the vector sum of the individual dipole moments. This is a reasonable approximation for many molecular situations including many peptides where extensive H-bonding is not important, such as individual β-strands and most small peptides. However, this approximation clearly breaks down where extended cooperative H-bonding becomes operative. For example, the dipole moments of H-bonding chains of acetic acid,[14] enols of 1,3-diones,[13] 4-pyridones,[6] formamides,[10] urea,[16] and α-helical peptides[11] all increase more then expected from the vector sums of their components as the chains grow. The reorganization of charge in response to an electric field is due to polarization, which is distinctly different as it is not static but is responsive to the magnitude of an applied electric field. More precisely, while the dipole moment is dE/dF, the polarizability is d^2E/dF^2 where E is the energy and F is the electric field. Unfortunately, many reports in the literature do not make the distinction between purely electrostatic interactions and those significantly due to polarizablity. When the electron density of a molecule becomes significantly polarized, the molecular geometry will necessarily relax to accommodate the change. In the chains of 4-pyridones considered in this paper, part of the geometry relaxation involves the lengthening of the C═O bonds. The effect of the lengthening of these C═O bonds can be observed in the correlation of the frequencies of the individually ^{14} C═O substituted pyridone monomers within the $(4\text{-pyridone})_9$ H-bonding chain. Similar effects have been observed for H-bonding formamide chains[17] and α-helical and β-sheet peptides.[43]

Hydrogen-bonding clearly is not always an entirely electrostatic interaction. Rather, it generally involves both polarization and covalent interactions.[44] For example, the observation that trans-hydrogen-bond scalar $^{13}C-^{15}N$ J-couplings can be measured indicates that spin information can be transferred across H-bonds. This cannot be accomplished through purely electrostatic interactions. Furthermore, the magnitude of these J-couplings is influenced by the existence of other H-bonds within a H-bonding chain as predicated by DFT calculations[45,46] and observed by experiments. Gilli has shown that H-bonds can be stabilized by resonance[47] to form what he calls resonance assisted H-bonds (RAHB's). Perhaps the clearest example of this phenomenon occurs in crystals of the enol of 1,3-cylcohexanedione,[48] in which the oxygens of two adjacent atoms are only 2.56 Angstroms apart.[49] The cyclic enol of acetylacetone provides another example. Here there is some controversy both in the theoretical[50−53] and experimental[54−56] literature as to whether the cyclic H-bond is truly symmetrical or slightly unsymmetrical. Even in the simple case of water dimer,

electrostatic interactions provide only a fraction of the stabilizing interaction that decreases as the H-bond becomes shorter.

The implications for the interpretation of the amide I bands of peptides are evident, if not entirely new.[57] Where chains of cooperative H-bonds are prevalent, the coupling of C═O's through the H-bonds should predominate over TDC. Through H-bond-coupling modifies the local geometries of the C═O's, thereby explaining the red-shifts of the amide I bands in α-helices and β-sheets (as well as the blue-shifts if the amide II bands, not discussed here). In fact, H-bonding aggregation of simple amides in solution has long been known to give rise to similar red-shifts.[58] This suggestion agrees with the experimental observations that the amide I bands of α-helices (which contain three chains of highly cooperative amide H-bonds[11]) are more red-shifted than those of unfolded peptide motifs, while those of β-sheets (which contain stronger and shorter[59,60] H-bonds than the helices) are even more red-shifted.

Conclusions

The coupling of both the amide-I and amide-A bands of H-bonded chains of 4-pyridones proceeds primarily via through H-bond coupling. These results, together with those already reported for formamide chains, suggest that similar coupling mechanisms for the amide-I bands of those domains of proteins and peptides that contain significant C═O···H−N cooperative H-bonding chains. The extensive polarizations caused by cooperative H-bonding chains induce geometric perturbations of the individual 4-pyridone monomers (particularly C═O bond-lengthening) that directly explain the large red-shifts of the amide-I bands, similar to those observed in α-helices and β-sheets of proteins and peptides.

Acknowledgment. This work was supported in part by funding form PSC-CUNY. Some of the computations were performed using the CUNY Graduate School research computing cluster.

References and Notes

(1) Whitesides, G. M.; Simanek, E. E.; Mathias, J. P. *Acc. Chem. Res.* **1995**, *28*, 37−44.
(2) Shi, X.; Barkigia, K. M.; Fajer, J.; Drain, C. M. *J. Org. Chem.* **2001**, *66*, 6513−6522.
(3) Brunet, P.; Simard, M.; Wuest, J. D. *J. Am. Chem. Soc.* **1997**, *119*, 2737−2738.
(4) Park, T.; Todd, E. M.; Nakashima, S.; Zimmerman, S. C. *J. Am. Chem. Soc.* **2005**, *127*, 18133−18142.
(5) Viswanathan, R.; Asensio, A.; Dannenberg, J. J. *J Phys. Chem. A* **2004**, *108*, 9205−12.
(6) Chen, Y.-f.; Dannenberg, J. J. *J. Am. Chem. Soc.* **2006**, *128*, 8100−1.
(7) Dannenberg, J. J. *Adv. Protein Chem.* **2006**, *72*, 227−73.
(8) Krimm, S.; Abe, Y. *Proc. Nat. Acad. Sci. U.S.A.* **1972**, *69*, 2788−92.
(9) Sheridan, R. P.; Lee, R. H.; Peters, N.; Allen, L. C. *Biopolymers* **1979**, *18*, 2451−8.
(10) Kobko, N.; Dannenberg, J. J. *J Phys Chem. A* **2003**, *107*, 10389−95.
(11) Wieczorek, R.; Dannenberg, J. J. *J. Am. Chem. Soc.* **2004**, *126*, 14198−205.
(12) Wieczorek, R.; Dannenberg, J. J. *J. Am. Chem. Soc.* **2003**, *125*, 8124−29.
(13) Turi, L.; Dannenberg, J. J. *J. Phys. Chem.* **1992**, *96*, 5819−24.
(14) Turi, L.; Dannenberg, J. J. *J. Am. Chem. Soc.* **1994**, *116*, 8714−21.
(15) Cardenas-Jiron, G. I.; Masunov, A.; Dannenberg, J. J. *J. Phys. Chem. A* **1999**, *103*, 7042-7046
(16) Masunov, A.; Dannenberg, J. J. *J. Phys. Chem. B* **2000**, *104*, 806−810.
(17) Kobko, N.; Dannenberg, J. J. *J. Phys. Chem. A* **2003**, *107*, 6688−6697.
(18) Torii, H.; Tatsumi, T.; Kanazawa, T.; Tasumi, M. *J. Phys. Chem. B* **1998**, *102*, 309−314.
(19) Ismer, L.; Ireta, J.; Boeck, S.; Neugebauer, J. *Phys. Rev. E* **2005**, *71*, 31911.
(20) Becke, A. D. *J. Chem Phys.* **1993**, *98*, 5648.
(21) Lee, C.; Yang, W.; Parr, R. G. *Phys. Rev. B* **1988**, *37*, 785.
(22) Frisch, M. J., et al. *GAUSSIAN 03*, Revision C01, Gaussian, Inc.: Pittsburgh, PA, 2003.
(23) Xiang, T.; Goss, D. J.; Diem, M. *Biophys. J.* **1993**, *65*, 1255−61.
(24) Diep, V.; Dannenberg, J. J.; Franck, R. W. *J. Org. Chem.* **2003**, *68*, 7907−10.
(25) Scott, A. P.; Radom, L. *J. Phys. Chem.* **1996**.
(26) Kobko, N.; Paraskevas, L.; del Rio, E.; Dannenberg, J. J. *J. Am. Chem. Soc.* **2001**, *123*, 4348−4349.
(27) Ham, S.; Kim, J.-H.; Lee, H.; Cho, M. *J. Chem. Phys.* **2003**, *118*, 3491−3498.
(28) Torii, H.; Tasumi, M. *J. Raman Spectrosc.* **1998**, *29*, 81−86.
(29) Mehler, E. L. *J. Am. Chem. Soc.* **1980**, *102*, 4051−6.
(30) Torii, H.; Tasumi, M. *AIP Conf. Proc.* **1998**, *430*, 719−722.
(31) Bour, P.; Keiderling, T. A. *J. Am. Chem. Soc.* **1993**, *115*, 9602−7.
(32) Bour, P.; Kubelka, J.; Keiderling, T. A. *Biopolymers* **2000**, *53*, 380−395.
(33) Kubelka, J.; Gangani, R. A.; Silva, D.; Keiderling, T. A. *J. Am. Chem. Soc.* **2002**, *124*, 5325−5332.
(34) Bour, P.; Keiderling, T. A. *J. Phys. Chem. B* **2005**, *109*, 5348−5357.
(35) Bour, P.; Kubelka, J.; Keiderling, T. A. *Biopolymers* **2002**, *65*, 45−59.
(36) Kubelka, J.; Keiderling, T. A. *J. Am. Chem. Soc.* **2001**, *123*, 12048−12058.
(37) Kubelka, J.; Keiderling, T. A. *J. Phys. Chem. A* **2001**, *105*, 10922−10928.
(38) Myshakina, N. S.; Asher, S. A. *J. Phys. Chem. B* **2007**, *111*, 4271−4279.
(39) Brauner, J. W.; Dugan, C.; Mendelsohn, R. *J. Am. Chem. Soc.* **2000**, *122*, 677−683.
(40) Huang, R.; Kubelka, J.; Barber-Armstrong, W.; Silva, R. A. G. D.; Decatur, S. M.; Keiderling, T. A. *J. Am. Chem. Soc.* **2004**, *126*, 2346−54.
(41) Hilario, J.; Kubelka, J.; Syud, F. A.; Gellman, S. H.; Keiderling, T. A. *Biopolymers* **2002**, *61*, 233−236.
(42) Cha, S.; Ham, S.; Cho, M. *J. Chem. Phys.* **2002**, *117*, 740−750.
(43) Viswanathan, R.; Wieczorek, R.; Dannenberg, J. J. Unpublished results, 2004−2006.
(44) Dannenberg, J. J.; Haskamp, L.; Masunov, A. *J. Phys. Chem. A* **1999**, *103*, 7083−7086.
(45) Salvador, P.; Kobko, N.; Wieczorek, R.; Dannenberg, J. J. *J. Am. Chem. Soc.* **2004**, *126*, 14190−7.
(46) Salvador, P.; Wieczorek, R.; Dannenberg, J. J. *J Phys. Chem. B* **2007**, *111*, 2398−2403.
(47) Bertolasi, V.; Gilli, P.; Ferretti, V.; Gilli, G. *J. Chem. Soc., Perkin Trans.* **1997**, *2*, 945−952.
(48) Gilli, G.; Bellucci, F.; Ferretti, V. *J. Am. Chem. Soc.* **1989**, *111*, 1023−8.
(49) Etter, M. C.; Urbanczyk, L. Z.; Jahn, D. A. *J. Am. Chem. Soc.* **1986**, *108*, 5871−6.
(50) Buemi, G. *J. Chem. Soc., Faraday Trans.* **1989**, *85*, 1771−8.
(51) Buemi, G.; Gandolfo, C. *J. Chem. Soc., Faraday Trans.* **1989**, *85*, 215−27.
(52) Dannenberg, J. J.; Rios, R. *J. Phys. Chem.* **1994**, *98*, 6714−18.
(53) Xu, S.; Park, S. T.; Feenstra, J. S.; Srinivasan, R.; Zewail, A. H. *J. Phys. Chem. A* **2004**, *108*, 6650−6655.
(54) Iijima, K.; Ohnogi, A.; Shibata, S. *J. Mol. Struct.* **1987**, *156*, 111−18.
(55) Lowrey, A. H.; George, C.; D'Antonio, P.; Karle, J. *J. Am. Chem. Soc.* **1971**, *93*, 6399−403.
(56) Caminati, W.; Grabow, J.-U. *J. Am. Chem. Soc.* **2006**, *128*, 854−857.
(57) De Loze, C.; Baron, M. H.; Fillaux, F. *J. Chim. Phys. Phys.-Chim. Biol.* **1978**, *75*, 631−49.
(58) Fillaux, F.; De Loze, C. *J. Chim. Phys. Physicochim. Biol.* **1972**, *69*, 36−44.
(59) Baker, E. N.; Hubbard, R. E. *Prog. Biophys. Mol. Biol.* **1984**, *44*, 97−179.
(60) Jeffrey, G. A.; Saenger, W. *Hydrogen Bonding in Bilogical Structures*; Springer-Verlag: Berlin, 1991.